Petroleum and Coal

Article **Open Access**

Investigating the Effect of Pyrolysis Parameters on Product Yields of Mixed Wood Sawdust in a Semi-Batch Reactor and its Characterization

Mohamed R. O. Ali, Ahmed Gaber H. Saif, Seddik S. Wahid

Dept. of Mechanical Power Engineering and Energy, Faculty of Engineering, Minia University, Minia 61519, Egypt

Received December 24, 2019; Accepted April 1, 2020

Abstract

A semi-batch pyrolizer has been designed and assembled to investigate the effect of various operating parameters on the product yields. Mixed wood sawdust was pyrolyzed to examine the temperature, particle size, and purge gas (N_2) flow rate effects on the yields of the products. Experiments at a temperature from 350 to 550°C with a step of 50°C have been carried out. Also, the particle size ranges of 0.25<Dp<0.5, 0.5<Dp<1, 1<Dp<2, and Dp>2 mm were used. The purge gas (N_2) flow rates of 100 to 500 cm^3/min with a step of 100 cm^3/min has been examined. The optimum pyrolysis conditions for the sawdust were 46 wt% at a temperature of 450°C, the particle size of 0.5<Dp<1 mm, and N_2 flow rate of 200 cm^3/min. For the products at optimum conditions, the elemental composition, HHV, viscosity, and density of the bio-oil was obtained. Several thermal and optical characterization of the sawdust, bio-oil, and biochar has been performed. The results showed that the bio-oil could be used as renewable fuel with an empirical formula of $CH_{1.27}O_{0.29}N_{0.009}$ and a higher heating value (HHV) of 28.45 MJ/kg. The bio-char could be used as solid fuels with a HHV of 35.43 MJ/kg and a feedstock to produce activated carbon for agricultural and industrial applications.

Keywords *Biomass; Sawdust; Pyrolysis; Product yield; Bio-oil; Bio-char.*

1. Introduction

Biomass to energy is rapidly becoming a key research area recently. The main advantages of renewable resources are that they contribute very little global warming potential, improve public health and environmental quality, and provide support for energy supply and sustainable adaptation to make the energy supply inexhaustible and resilient. Currently, biomass was continuously considered as a prospective source for the production of several fuels, chemicals, and other byproducts [1]. Several types of biomass feedstocks have been investigated like forestry residuals [2-5], wastes of agricultural crops [6-8], organic solid wastes from food processing [9-11], recycled paper [12], municipal solid wastes [13-14], and aquatic plants [15-16]. The potential availability of biomass makes it a suitable solution for the energy crisis.

The major techniques for the thermochemical conversion of biomass are combustion, gasification, pyrolysis, and torrefaction. Technically, the key aspects that determine the type of process are the desired end-product, economic conditions, pollution emission, and the specific factors for the project [17]. Among them, the pyrolysis process is simply a thermal conversion processes in the absence of oxygen, where the biomass decomposes to bio-oil (desired product), biochar (raffinate), and non-condensable gas (by-product). The percentage of each pyrolysis product depends on the process parameters as well as the feedstock composition. The key parameters are the operating temperature, heating rate, feed particle size, residence time, and the flow rate of sweeping gas (N_2) [18]. To get a significant yield of bio-oil, it is vital to control these parameters within the desirable range.

Many researchers have investigated the pyrolysis parameters for various wood wastes and forestry residuals and agricultural wastes, such as wood sawdust and orange bagasse. Varma *et al.* [19] investigated the effect of pyrolysis parameters for sawdust pyrolysis on the bio-oil

yield in a semi-batch fixed-bed reactor. The temperature of pyrolysis and heating rate were ranged from 350 to 650°C and 10 to 50°C/min, respectively. The particle size was varied in the range of 0.25 to 1.7 mm and purge gas (N_2) flow rate from 50 to 200 cm^3/min. The result shows that the maximum bio-oil yield was 44.16 wt%, obtained at 500°C, the heating rate of 50°C/min, the particle size of 0.6<Dp<1 mm, and nitrogen flow rate of 100 cm^3/min. This bio-oil has a calorific value of 27.82 MJ/kg and an empirical formula of $CH_{1.94}O_{0.71}N_{0.007}$. In another work, a semi-batch reactor with a feedstock of orange bagasse has been investigated by Bhattacharjee and Biswas [20]. They studied the effect of pyrolysis temperature, heating rate, and purging gas (N_2) flow rate on product yields and their characterization. The highest oil yield of 35.53 wt% was obtained at pyrolysis temperature of 525°C, the particle size of 0.425 mm, with a heating rate of 75°C /min and a sweep gas flow rate of 200 cm^3/min (N_2) with a calorific value of 21.72 MJ/kg and empirical formula of $CH_{1.33}O_{0.55}$. Salehi *et al.* [21] presented the effect of the operating conditions on the yield of the pyrolysis process in a fixed-bed reactor. They indicated that the yield reached 45 wt% of the raw material. Similarily, Demirbas [22] performed a pyrolysis process for the sawdust of the beech wood to calculate the yield as a function of the temperature of pyrolysis and moisture content of the sawdust. He proved the increase of the yield of liquid products as a function of temperature and moisture content. The liquid yield was 33%, with a moisture content of 54.8%. Aguado *et al.* [23] studied the effect of pyrolysis temperature on the yield in a spouted bed reactor using a sample of sawdust. They found that the liquid yield was 70 wt % obtained at a temperature of 450°C.

The research to date has tended to focus on the parameters rather than the semi-batch reactor design. In the present study, the pyrolysis of mixed wood sawdust is carried out in the reactor. The effects of pyrolysis temperature, purge gas flow rate, and particle size range on the pyrolysis yield have been studied. In addition, the characteristics of the feedstock, bio-oil, and bio-char have been performed to verify the chemical composition of the products. In addition, biogas is analyzed, and a discussion of the different methods for utilization of pyrolysis products as a potential source of renewable fuel and chemical feedstock is presented.

2. Material and methods

2.1. Raw materials

Mixed wood sawdust (pine and beech wood sawdust) was obtained from a lumber mill, which represents a waste product of woodworking operations. It was screened to the size range of 0.25<Dp<0.5, 0.5<Dp<1, 1<Dp<2, and Dp>2 mm with the help of a standard sieve (Zhejiang Tugong instrument Co). The biomass feedstock was dried at 100°C for 24 hours before each experiment to remove the moisture content. Table 1 shows the ultimate and proximate analysis of the sawdust sample.

Table 1. Main characteristics of the mixed wood sawdust

Characteristics	Sawdust	Method
	Proximate analysis (wt%)	
Moisture content	2.83	ASTM D-7582
Volatile matter	78.92	ASTM D-7582
Ash content	1.78	ASTM D-7582
Fixed carbon	16.47	ASTM D-7582
	Ultimate analysis (wt%)	
Carbon (C)	48.7	ASTM D-5373
Hydrogen (H)	6.04	ASTM D-5373
Nitrogen (N)	0.94	ASTM D-5373
Sulfur (S)	0.3	ASTM D-4294
Oxygen (O)	43.99	By difference
O/C molar ratio	0.68	Calculation
H/C molar ratio	1.49	Calculation
Empirical formula	CH1.49 O0.68 N0.017	Calculation
HHV (MJ/kg)	19.21	ASTM D-240

2.2. Methods for characterization

Proximate analysis of sawdust and bio-char were performed to determine the moisture content, volatile matter, ash, and fixed carbon contents consistent with the ASTM standards [24]. The ultimate analysis (CHNS analysis) of feedstock and the products has been done to determine the carbon (C), oxygen (O), hydrogen (H), nitrogen (N), and sulfur (S) content. It was tested by the macro combustion analyzer provided by Vario macro Cube, Germany.

The HHV of sawdust, bio-oil, and biochar was performed in a Parr 6200 Bomb calorimeter, according to ASTM D-240. ASTM standard methods were used to determine the physical properties of bio-oil, such as kinematic viscosity and water content. The water content was determined by the Karl-Fischer titration in line with ASTM D-6304. The pH of bio-oil was measured according to ASTM D-664.

The organic functional groups exist in sawdust, bio-oil, and biochar were determined using a BRUKER Vertex 70 FTIR spectrometer. Typically, pellets of dried bio-char and KBr are prepared by pressing under vacuum. While for the bio-oil, a small drop of sample is put on the KBr pellet and then analyzed. The FTIR spectrum for sawdust, bio-oil, and biochar has been developed at a wavenumber range of 4000-400 cm^{-1}.

Gas Chromatography-Mass Spectrometry (GC-MS) analysis of bio-oil has been performed using an Agilent 7890A Gas Chromatography (GC) equipped with an Agilent 5975 Inert Mass Spectrometry (MS) with a triple-axis detector, using a (0.25 mm × 30 m) HP-5MS capillary column with 0.25 µm film thickness to identify the volatile compounds exist in the bio-oil. The heating process was programmed as follows: start at 25°C, then increase to 50°C and hold for 5 min, then heating to 280°C at a rate of 6 °C/min. Injector and detector temperatures were 250°C and 230°C, respectively. The MS was kept at 70 eV ionization energy with a mass electron (m/z) range of 50-550. The injection process has been done with a split-less mode to inject 1 µl sample solution. Helium was used as a carrier gas with a flow rate of 1 ml/min. The sample was diluted with hexane before injection. Compounds were identified using the NIST library of mass spectra database.

The gaseous products were collected in gas sample bags and analyzed by GC (VARIAN CP-3800 gas chromatograph) to determine the gas composition. The device is equipped with a Flame Ionization Detector (FID), a stainless-steel column (2.0 m x 1/8 inch I.D), and a molecular sieve 13X (80-100 mesh) operating in backflush mode at 50°C.

The X-Ray Diffraction (XRD) analysis of sawdust and biochar were performed in a PANalytical Empyrean X-Ray Diffractometer (model 202964) operating at 40 kV and 30 mA with a scan rate of 2°/ min using copper CuKα radiation source (λ =0.154nm) in the range of 5° to 80°.

The shape of the sawdust and biochar surfaces have been investigated using a scanning electron microscope (SEM) (JCM-6000 Plus) that has an acceleration voltage of 15 kV and equipped with Energy-Dispersive X-Ray Spectrometer (EDX).

3. Experimental setup and procedure

The following section describes the experimental apparatus set up and the procedure of the set of the experiment that was carried through this piece of work.

3.1. Experimental setup

Figure 1 shows the experimental setup, which consists of a cylindrical semi-batch reactor equipped with an electrically heated furnace, a condensation system, a nitrogen gas cylinder, a PID controller, and biomass feeding and char removing system. The reactor was made of stainless steel 304 with an inner diameter of 100 mm and a length of 0.4 m. The reactor was externally heated using the electric furnace (2.5 kW power), which is insulated to reduce the heat loss. A K-type thermocouple was inserted inside the reactor to measure the pyrolysis temperature. A PID controller has been used to control the temperature inside the reactor. The N_2 cylinder was used to supply N_2 gas to create an inert condition inside the pyrolizer. The reactor was connected to three condensers (one stainless steel and two glass condensers). The condensed liquid was collected at the end of each condensation stage in a collecting flask

and then weighted to get the yield. The first condenser flask was kept at zero °C. The feeding system consists of feeding hopper, screw feeder, and water-cooling jacket to prevent the decomposition of biomass before the heating zone. After the pyrolysis process, the reactor was left to cool, and char was removed from the reactor by using a screw system, then collected and weighted. The weight of non-condensable gases was calculated by mass balance as the difference between the total biomass feed and the sum of liquid and char yield.

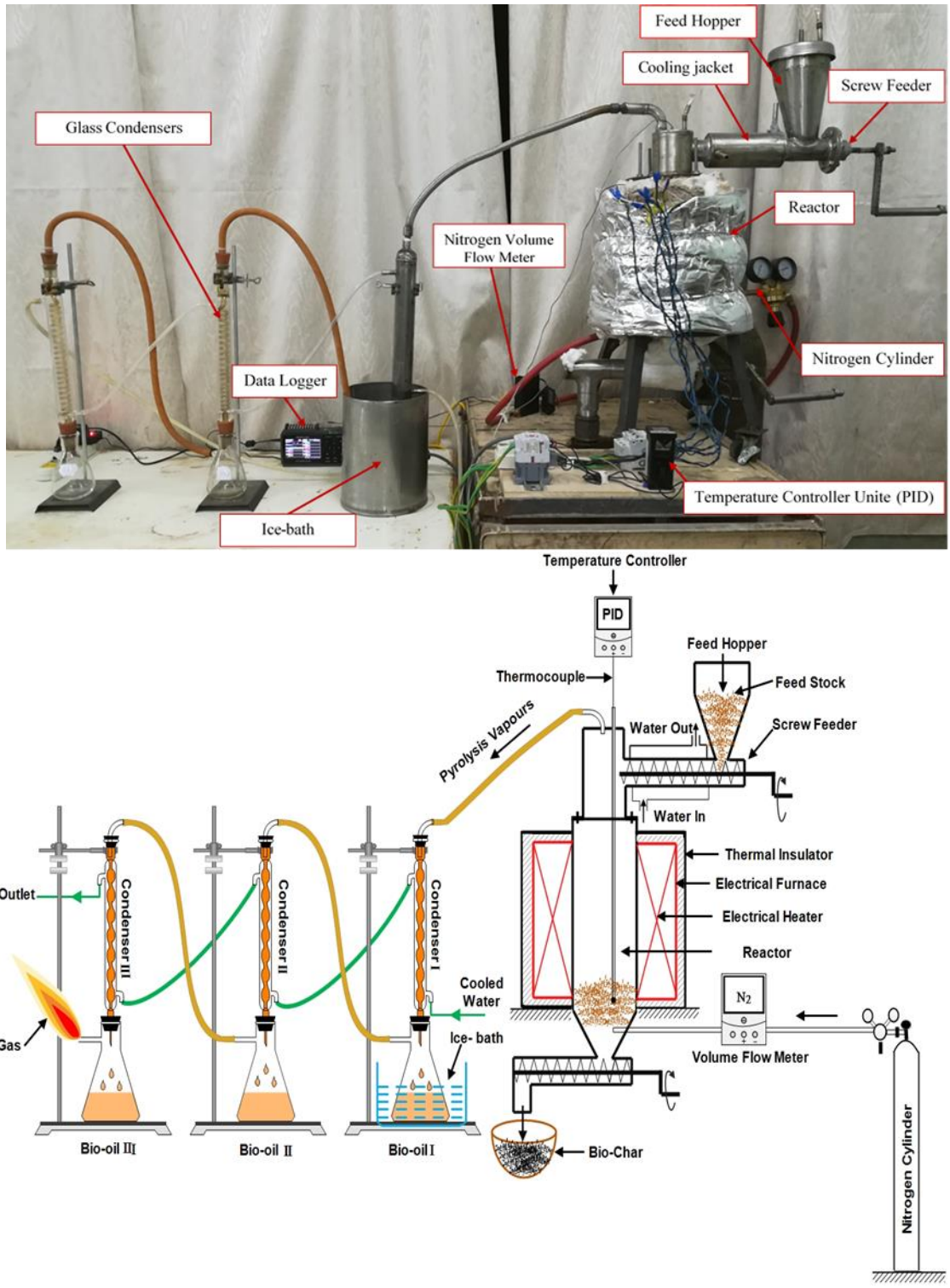

Fig. 1 Schematic diagram of the experimental set-up

3.2. Experimental procedure

The pyrolysis experiments have been performed in three sets. In all experiments, 100 g of biomass sample was put into the biomass feeding hopper. After the reactor reached the desired temperature, the biomass is dropped down into the reactor using the screw feeder. Before each experiment, nitrogen was purged inside the reactor with a flow rate of 200 cm^3/min for 15 min to create an inert condition inside the reactor.

The temperature was the studied parameter in the first set of experiments. After achieving the required temperature, a dried sawdust sample with a particle size of 0.5<Dp<0.1 mm was supplied to the reactor. The temperature was maintained at a set value of 350°C to 550°C, and the flow rate of N_2 was constant at 200 cm^3/min. At each final temperature, the experiment was adjusted to the set temperature and continued for additional 30 minutes to ensure that the total conversion of biomass or until no significant release of brown gas has been noted at the reactor outlet.

The second studied variable was the particle size and its effect on the distribution of the product. All experiments were performed with different particle0.25<Dp<0.5, 0.5<Dp<1, 1<Dp<2, and Dp>2 mm. For all experiments, the pyrolysis temperature and N_2 flow rate were 450°C and 200 cm^3/min, respectively.

The third studied parameter was the sweeping gas (N_2) flow rate. The nitrogen flow rate varies from 100 to 500 cm^3/min. For all pyrolysis experiments, the final pyrolysis temperature and the particle size were 450°C and 0.5<Dp<0.1 mm, respectively, based on the results of the first and second groups of experiments.

4. Results and discussion

4.1. Characterization of raw material

Table 1 summarizes the ultimate and proximate analysis, the HHV, and the empirical formula of sawdust. Proximate analysis is used to explore the fuel quality and good indication of the burning and heating properties of solid biomass [25]. It is worth mentioning that the moisture content in the pyrolysis process should be less than 10% because as the moisture content increases, additional heat should be supplied to remove the moisture and reduces the decomposition efficiency of biomass [26]. Due to the high volatile matter with low ash and moisture content, biomass is more suitable for the pyrolysis process. Forest biomass samples have much lower ash content and higher volatile matter compared with agricultural wastes [27].

From Table 1, the sawdust exhibited a high volatile percentage, which indicates the suitability of sawdust to be devolatilized and to reach high bio-oil yield. The ash content of 1.78% is low, and this is favorable for the pyrolysis process because the high ash content in biomass has a bad effect on the thermochemical conversion process and increase of slag formation problems, fouling and corrosion in pyrolysis reactors [28]. Fixed carbon content in the sawdust calculated by difference, is 16.47%. Ultimate analysis of sawdust shows the C, H, O, N, and S contents are 48.7, 6.04, 43.99, 0.97, and 0.3%, respectively. This result shows that S and N contents are low, so the sawdust contains lower the amount of sulfur oxides (SO_x) and nitrogen oxides (NO_x) during pyrolysis. The empirical formula of sawdust is found to be $CH_{1.49}O_{0.68}N_{0.017}$ calculated from the ultimate analysis data. The Hydrogen to Carbon (H/C) and Oxygen to Carbon (O/C) molar ratios of present sawdust are found as 1.49 and 0.68, respectively. The HHV is a fuel property of biomass that is used to evaluate the potential thermal energy content of biomass during pyrolysis. The HHV of sawdust is 19.21MJ/kg. The above analysis of sawdust shows that it has the potential for use as feedstock for the pyrolysis process.

The FTIR analysis is used to identify the characteristic functional group and chemical constituents in the raw material samples, which is essential for determining the composition and distribution of products in the pyrolysis process [29]. FTIR analysis is typically used to verify the appearance of cellulose, hemicellulose, and lignin in the biomass samples. Figure 2 depicts the FTIR curves of the sawdust feedstock. A deep peak at 3341 cm^{-1} corresponding to the O-H stretching, which is related to the presence of both carbohydrates and lignin [30]. Usually,

the bands in the range of 2800-3000 cm^{-1} are related to the C-H stretching along with CH aliphatic vibration. The band at 2890 cm^{-1} denoted the symmetric stretch of the CH_3 functional group. This indicates the presence of cellulose, hemicellulose, and lignin [31]. The band at 1725 cm^{-1} is due to the stretching vibration of the C=O bond, which the characteristic of carbonyl group appearing due to the presence of hemicellulose [32]. The peak around 1651 cm^{-1} is referred to as the C-C stretching vibration of aromatic, which corresponds to lignin [33]. The band at 1432 cm^{-1} is probably due to the bending vibration of the C-H bond in cellulose and hemicellulose [34]. The peaks between 1200 and 900 cm^{-1} are denoted to the C-O, C-C, C-O-C stretching, and C-OH bending vibrations of polysaccharides, which also appears in the cellulose and hemicellulose [33]. The bands between 1000-1400 cm^{-1}, due to the combination and overlap of C-O stretching bands, as well as various deformations. The existence of various functional groups in the sawdust, as outlined in Fig.2, proves the possibility of emerging gases like CO, CO_2, CH_4, H_2, and C_nH_m during the pyrolysis process. Similar types of FTIR spectra have been reported for sawdust and other biomass, such as pine sawdust [35-36], coffee husks, rice husks, tucuma seeds [37], palm kernel shell, empty fruit bunches and palm mesocarp fiber [33], corn stalks and pine sawdust [38], poplar sawdust [39], palm oil waste [40].

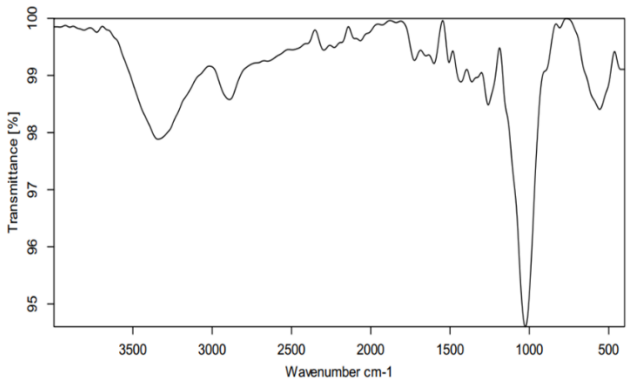

Fig. 2 FTIR spectra of sawdust

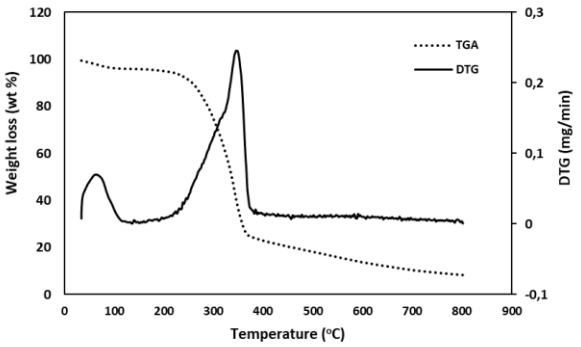

Fig. 3 TGA/DTG curves of sawdust at a heating rate of 10°C/min

Thermogravimetric analysis (TGA) is the best technique to recognize the behavior of pyrolysis of biomass used at a low heating rate [41]. The thermal performance of the sawdust feedstock has been conducted using differential TGA at a heating rate of 10°C/min starting from 34°C to 800°C. Figure 3 shows the TGA and derivative thermogravimetric (DTG) curves of the sawdust. It is noted from the curves of TGA and DTG that sawdust degradation is divided into three stages. The first stage of thermal degradation starts from a temperature of 35°C to 175°C, in which 3.5 % of weight loss occurs due to the removal of moisture in the sawdust sample. It is also shown by the DTG curve that the rate of weight loss is 0.07 mg/min at 65°C. The second stage starts from a temperature range of 175°C to 378°C, with a maximum weight loss of 72%. For this stage, the DTG curve also shows a peak with a maximum rate of weight loss of 0.25 mg/min at 345°C. During this stage, the mass loss is caused by hemicellulose and cellulose degradation. This section is recognized as the active pyrolysis zone due to the high rate of mass loss [42]. The third stage happens with a negligible weight loss in the range of 378°C to 800°C. This is mainly due to the decomposition of lignin that happens slowly over a wide temperature range and results in more solids (char) than volatiles [43]. From the TGA and DTG curves, the ideal temperature range for pyrolysis and bio-oil production is about 350-500°C.

4.2. Effect of the operating parameters

The operating parameters addressed in this section are: pyrolysis temperature, sweeping gas flow rate, and particle size of biomass.

4.2.1. Effect of pyrolysis temperature

Temperature is considered to be the most significant parameter affecting the distribution yields of the pyrolysis product. In the pyrolysis process, the principal function of temperature is to supply the required heat for the decomposition of biomass bonds. The biomass conversion process increases with increasing the pyrolysis temperature; this is due to an increase in energy to break the biomass bonds. Figure 4 shows the product yield distribution for pyrolysis of sawdust with pyrolysis temperatures of 350, 400, 450, 500 and 550°C, for the biomass particle size of 0.5<Dp<1 mm with N_2 flow rate of 200 cm^3/min. As shown in Figure 4, the yield of bio-oil increases as the temperature increases until it reaches a peak at 450°C and thereafter decreases. A maximum bio-oil yield of 46 wt% is found at a pyrolysis temperature of 450°C, which is in line with previous works [3, 19]. The decrease in the yield of bio-oil after 450°C is probably due to secondary cracking reactions of the volatiles, resulting in higher gas yield as well as secondary char decomposition. This increases gaseous products; therefore, liquid yield decreases [44]. Figure 4 shows that the biochar yield decreases from 37 wt% to 25 wt%, whereas the gas yield increased from 24 wt% to 34 wt% as temperature increases from 350°C to 550°C. As pyrolysis temperature increases, the bio-char yield decreased because of the secondary decomposition of char at the higher temperature.

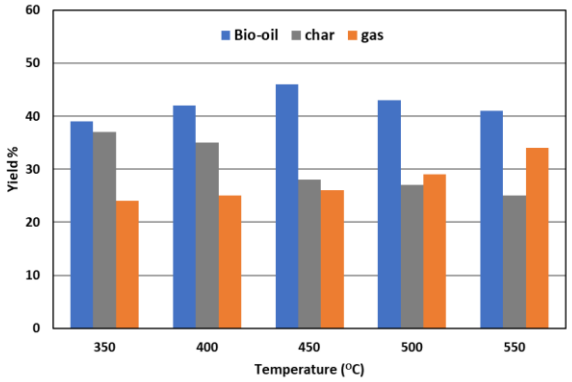

Fig. 4. Effect of pyrolysis temperature on product yields at particle size of 0.5<Dp<1 mm and nitrogen flow rate of 200 cm^3/min

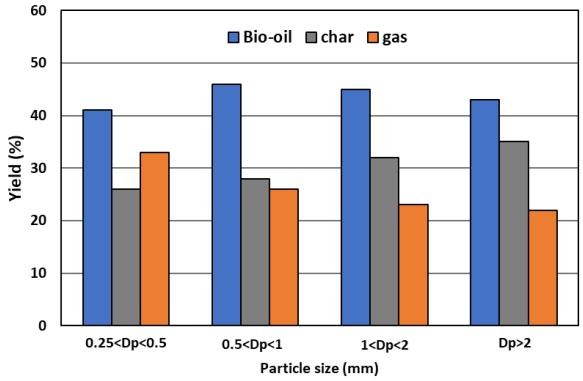

Fig. 5. Effect of particle size on the product yields at temperature of 450°C and nitrogen flow rate of 200 cm^3/min

4.2.2. Effect of particle size

Figure 5 shows the effect of sawdust particle size on the product yields at a constant pyrolysis temperature of 450°C and sweeping gas (N_2) flow rate of 200 cm^3/min. For a particle size Dp<0.5mm, the bio-oil yield is found as 41 wt%, and for the larger particle size of Dp >2 mm, the bio-oil yield is found as 43 wt%. The difference in bio-oil yield for smaller and larger particle sizes is only 2%. So, the particle size has an insignificant effect on bio-oil yield. The small differences in the obtained results are probably due to experimental errors. However, the biochar yield increases from 26 wt% to 35wt%, whereas gas yield decreases from 33 wt% to 22 wt% as the particle size increases from Dp<0.5 mm to the range of Dp>2 mm. This occurs because, for larger size particles, greater gradients exist inside it so that at a given moment, the core temperature is lower than that of the surface. This possibly decreases the bio-oil and gaseous product yields and increase the char yield [48]. Similar results from the pyrolysis of various types of biomass have been obtained [19]. The thermal conductivity of sawdust is very low (0.052 W/mK), which leads to poor heat distribution through the pyrolizer. It is well known that the thermal conductivity of biomass is very low and is classified as a poor heat conductor that poses difficulties in heat transfer during pyrolysis. The influence of the particle size of biomass on product yields is considered important. The useful particle size of biomass for pyrolysis depends upon the type of pyrolizer, pyrolysis process, and nature of biomass. Commonly, small particle size is favored in the pyrolysis process because of uniform and fast heating that leads to producing higher volatile matter. Dissimilarly, large particle size

will generate a temperature gradient inside the particle, leading to a reduced heat transfer. Consequently, the bio-char yield should increase, and the bio-oil and bio-gas yield will decrease. Additionally, larger particle sizes will acquire higher values of activation energy, which hider the decomposition reaction [45].

4.2.3. Effect of sweeping gas (N_2) flow rate

The flow rate of inert gas is very important in the pyrolysis process. As N_2 gas is inert at a moderate temperature, it can be used to create an inert atmosphere inside the pyrolizer. Also, N_2 gas carries away the pyrolysis gases, thus, decreasing its residence time in the hot zone. Furthermore, as the pyrolysis gases sweep away from the reaction zone, the side reactions will be kept minimum, enriching the production of the bio-oil [46]. Therefore, fast separation of pyrolysis vapor from the reaction zone is vital to improve the production yield and to hider the side reactions [42].

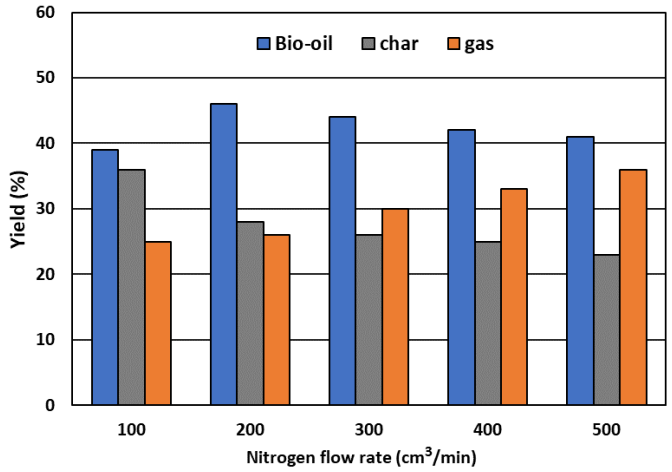

Fig. 6. Effect of nitrogen flow rate on product yields at pyrolysis temperature of 450°C and particle size of 0.5<Dp<1 mm

Figure 6 depicts the effect of the flow rate of the N_2 gas on the products yield at a pyrolysis temperature of 450°C and the particle size of 0.5<Dp<1 mm. It is evident that the bio-oil yield increases from 39 wt% to 46 wt%, by increasing the N_2 flow rate from 100 to 200 cm^3/min. But when the flow rate increases to 500 cm^3/min, the bio-oil yield decreases back to 41 wt%. Also, the char yield decreases from 36 % to 23 % and gas yield increases from 25 wt% to 36 wt%.

A possible explanation for these results may be that at high flow rate of N_2, poor condensation of the vapors associated with N_2 stream is expected [47]. In addition, as the N_2 flow rate increases from 100 to 500 cm^3/min, poor heating of the feedstock is expected inside the pyrolizer; therefore, lower bio-oil and biochar yield are expected. So, it is evident that char yield decreases and the gas products yield increases with the N_2 flow rate. Similar observations in the literature have been reported [22].

4.2.4. Characterization of bio-oil

The energy content of fuel depends principally on the content of hydrogen and carbon, so it's significant to determine the ultimate analysis of bio-oil. For the present study, C and H contents in bio-oil are 66.28 and 6.98 %, respectively, whereas 48.7 and 6.04%, for sawdust, respectively. This shows that the content of H and C in the bio-oil is more than in the biomass. The content of oxygen in bio-oil (25.94%) is lower than that of the original raw material (43.99%). It is vital to reduce the oxygen content because it yields a fuel with high calorific value. The values of N and S content in the sawdust bio-oil are low as 0.76 and 0.04%, respectively. Consequently, this bio-oil is favorable for fuel application because the higher amount of N and S in the fuel produces nitrogen oxides (NOx) and sulfur oxides (SOx) during combustion, which are responsible for environmental pollution. The H/C and O/C molar ratios of sawdust bio-oil is 1.264 and 0.293, respectively. In bio-oil, the H/C molar ratio is lower than light and heavy crude oils (1.5-1.7). The H/C ratio for transportation fuel should be increased within the range of 1.9-2.0. So, upgrading bio-oil can be by increasing this ratio by adding hydrogen using hydrotreating [48]. The molar ratio of H/C should be high, and O/C should be low for the promising use of bio-oil for energy application. The empirical formula of sawdust bio-oil obtained from elemental analysis data is $CH_{1.27}O_{0.29}N_{0.009}$. For evaluating and

determining the feasibility of bio-oil as a fluid fuel, physical and fuel characteristics such as density, kinematic viscosity, water content, pH, and calorific value of bio-oil are essential. Bio-oil from Sawdust is dark brown in color and smoky. The density of sawdust bio-oil is determined as 1085 kg/m^3 at 15 °C, which is similar to the other bio-oil obtained from different raw material like wood sawdust [19], pinewood [36], wood wastes [14] and sweet lime empty fruit bunch [49]. The liquid fuel viscosity is an important parameter in the design and operation of the fuel injection system. The present bio-oil has a kinematic viscosity of 10.54 cSt at 40°C, which is high as compared to the conventional fuel. Because of high density and viscosity, the pumping and atomization of bio-oil in engine may be difficult and affect the combustion quality of bio-oil. So that the bio-oil upgrading and refining are required to obtain the desired quality like diesel and heavy fuel oil. The bio-oil pH is 3.4. It is acidic in nature due to the existence of organic acids, phenols and aldehydes. Bio-oil is highly unstable and corrosive for aluminum and mild steel due to its low pH value [50]. Bio-oil water content is 300 ppm. The HHV of sawdust bio-oil is 28.45 MJ/kg, which is comparable to the other pyrolytic oils [51-52]. However, it is lower than the commercial diesel (42-45 MJ/kg) because it contains more oxygen content than petroleum fuel.

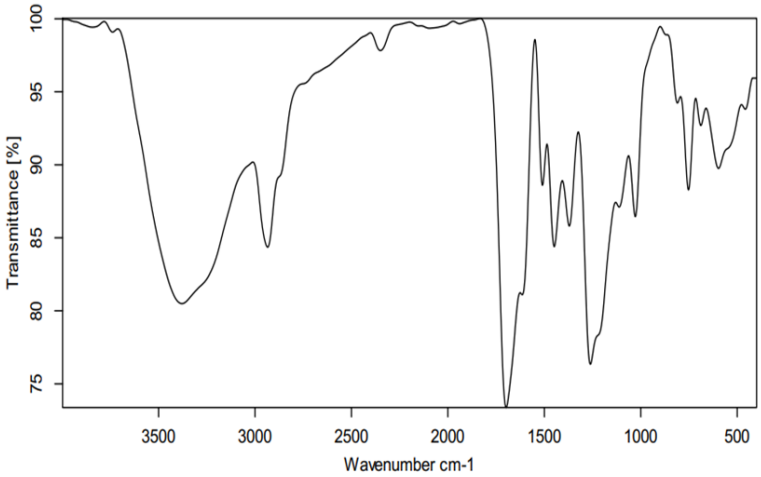

Fig. 7. FTIR spectra of bio-oil

Figure 7 shows the bio-oil FTIR spectrum. It provides information about the presence of several functional groups and chemical bonds. The O-H vibrations of the bio-oil lie between 3200 and 3600 cm^{-1} imply the existence of alcohols and phenols [12]. The C-H stretching vibration bond is found between 2800 and 3000 cm$^{-1,}$ and C-H stretching and bending vibrations is between 1350 and 1465 cm^{-1}, which indicate the presence of alkane [53-54]. The appearance of the peak at 1509 cm^{-1} represents C-C stretching vibration, which indicates the existence of alkenes and aromatics [54]. The C-O stretching vibrations peak is found between 1100-1300 cm^{-1}, which indicates the presence of carboxylic acid or ester. The region from 600 to 900 cm^{-1} implies the presence of C-H bending aromatic compounds. Furthermore, the peaks in the range of 800-1000 cm^{-1} are connected to the presence of alkanes and amines. The FTIR results of sawdust bio-oil are in line with other results obtained by the previous studies [55-57].

In addition, the bio-oil was analyzed by GC-MS to quantify the presence of various chemical components/groups in the bio-oil and to justify the existence of the aforementioned functional groups. The GC-MS analysis of the pyrolytic oil demonstrates the chemical compounds present in bio-oil. Compounds from the chromatogram were recognized in comparison with the library database of the National Institute of Standards and Technology (NIST). The GC-MS chromatograph indicates that more than 30 peaks have been obtained, but it is not possible to separate all peaks due to the complex nature of bio-oil and, limiting the strength of the MS library. Figure 8 shows the bio-oil GC-MS spectrum, and Table 2 shows the list of bio-oil components that have a peak area of more than 3 % with their retention time, peak area percentage,

compound name, and molecular formula. The GC-MS results show the presence of Aliphatic and aromatic furans, acids, alcohols, hydrocarbons, phenols, and oxygenated compounds are in the bio-oil. The most significant compounds in the bio-oil are furfural (9.842%), phenol, 2-methyl (6.091%), phenol, 3-methyl (9.087%), phenol, 2-methoxy (11.804%), phenol,2,4-dimethyl (15.807%), creosol (7.942%), phenol, 4-ethyl-2-methoxy (6.082%) and retene (6.383%) as shown in Table 2.

Table 2. Main compounds identified in bio-oil

RT (min)	Compound name	Formula	Peak area (%)
3.533	Toluene	C_7H_8	4.464%
4.036	Dodecane	$C_{12}H_{26}$	4.164%
5.225	Furfural	$C_5H_4O_2$	9.842%
7.696	2-Cyclopenten-1-one, 2-methyl	C_6H_8O	4.151%
7.788	2-Pentanol, 5-methoxy-2-methyl	$C_7H_{16}O_2$	5.397%
9.427	Benzaldehyde	C_7H_6O	5.437%
12.529	Phenol, 2-methyl	C_7H_8O	6.091%
13.170	Phenol, 3-methyl	C_7H_8O	9.087%
13.386	Phenol, 2-methoxy	$C_7H_8O_2$	11.804%
15.107	Phenol, 2,4-dimethyl	$C_8H_{10}O$	15.807%
16.164	Creosol	$C_8H_{10}O_2$	7.942%
18.287	Phenol, 4-ethyl-2-methoxy	$C_9H_{12}O_2$	6.082%
35.493	Retene	$C_{18}H_{18}$	6.383%
40.396	7-Oxodehydroabietic acid, methyl ester	$C_{21}H_{28}O_3$	3.350%

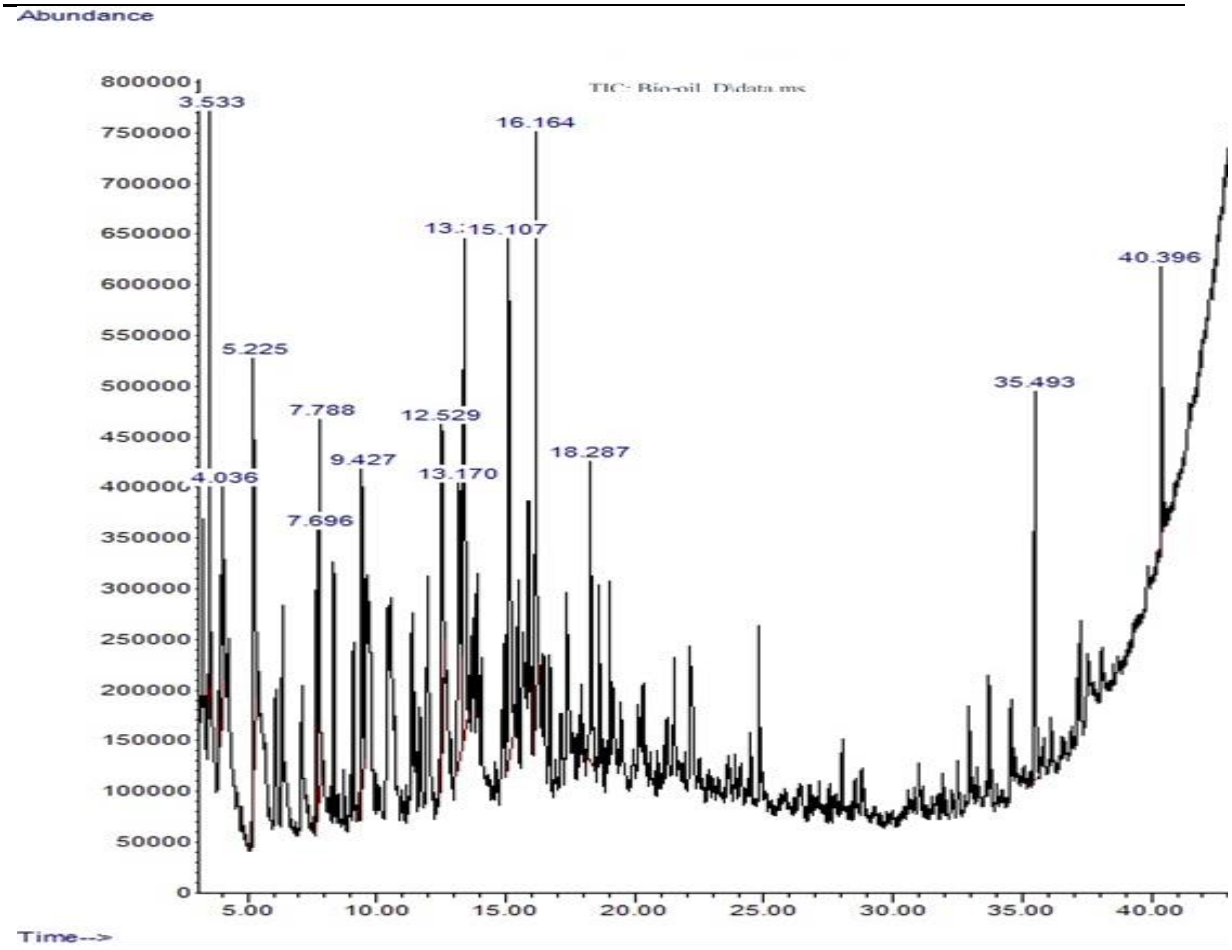

Fig. 8. GC-MS chromatogram of bio-oil

4.2.5. Gas chromatographic analysis of pyrolytic gas

Product gas composition released during the pyrolysis of sawdust is determined by Gas Chromatograph (GC). Gases released during pyrolysis of sawdust at 450°C, consist of methane (CH_4), carbon dioxide (CO_2), carbon monoxide (CO), low carbon number hydrocarbons such as ethylene (C_2H_4), and ethane (C_2H_6), propylene (C_3H_6), propane (C_3H_8) and small amounts of other gases as shown in Table 3. Pyrolysis gas can be used in various applications such as heat or electricity production and the production of individual gas products, including CH_4, H_2, or other volatiles, or in the production of liquid fuels through synthesis. In some applications, it can be used to preheat the inert carrying gas or can be returned to the pyrolysis reactor as a sweeping gas.

Table 3. Pyrolytic gas composition

Components	Mol %	Wt%
Methane (CH_4)	10.99	5.74
Carbon mono Oxide (CO)	61.10	55.57
Carbon dioxide (CO_2)	24.60	35.15
Ethylene (C_2H_4)	1.59	1.45
Ethane (C_2H_6)	0.82	0.79
Propylene (C_3H_6)	0.58	0.79
Propane (C_3H_8)	0.18	0.25
Butylene (C_4H_8)	0.12	0.22
Iso-butane (C_4H_{10})	0.01	0.02
Normal- butane (C_4H_{10})	0.01	0.02
Density g/L @NTP	1.0634	
Average molecular weight	30.793	

4.2.6. Characteristics of biochar

Bio-char produced by biomass pyrolysis is a brilliant source for energy, and one of its uses is to be used as a solid fuel; also, it can be used as a bio-sorbent, soil amendment. It can also be used for activated carbon and value-added product production. So, various characteristics of biochar have been done to detect its potential for applications through a suitable route, as mentioned above. Table 4 lists the characterization of sawdust bio-char.

Table 4. Characteristics of the sawdust bio-char

Characteristics	Bio-char	Method
	Proximate analysis (wt%)	
Moisture content	1.65	ASTM D-7582
Volatile matter	16.53	ASTM D-7582
Ash content	14.25	ASTM D-7582
Fixed carbon	67.57	ASTM D-7582
	Ultimate analysis (wt%)	
Carbon (C)	75.87	ASTM D-5373
Hydrogen (H)	6.2	ASTM D-5373
Nitrogen (N)	1.04	ASTM D-5373
Sulfur (S)	0.03	ASTM D-4294
Oxygen (O)	16.86	By difference
O/C molar ratio	0.17	Calculation
H/C molar ratio	0.98	Calculation
Empirical formula	$CH_{0.98}O_{0.17}N_{0.012}$	Calculation
HHV (MJ/kg)	35.43	ASTM D-240

The moisture content of bio-char is 1.65% because of the bio-char absorbs some moisture when it is exposed to air. The volatile matter of sawdust is 78.92%, which significantly reduces to 16.53% after pyrolysis. It is due to the conversion of volatile matter into gaseous and liquid products because of decreasing in volatile matter content, and the fixed carbon content increases to 67.57%. Ash content in bio-char is 14.25%. The ultimate analysis result shows that

bio-char becomes carbonaceous with the carbon content of 75.87%. From Tables 1 and 4, it is observed that there are significant variations in oxygen and carbon content and slight variations in nitrogen, sulfur, and hydrogen content between sawdust and their bio-char. The bio-char has a lower oxygen content and higher carbon content as compared to sawdust. This signifies that the increases in the carbon content are due to the removal of oxygen and other volatile compounds [58]. The N and S contents in bio-char are low as 1.04 and 0.03%, respectively.

The biochar H/C and O/C molar ratios are lower than the original biomass. It indicates a loss of H and O due to decarbonylation, decarboxylation, and dehydration during pyrolysis [59]. Although the heating value of bio-char (35.43 MJ/kg) obtained is high when compared with original biomass (19.21 MJ/kg). The empirical formula of bio-char is found as $CH_{0.98}O_{0.17}N_{0.012}$. The preceding analysis of bio-char suggests that it embraces the potential to be utilized as solid fuel.

Figure 9 shows the bio-char FTIR spectrum. The peaks present in spectra between 800 and 1000 cm^{-1} are due to aromatic C-H stretching vibrations that indicate the existence of adjacent aromatic hydrogens in bio-chars [7]. The peaks between 1000-1200 cm^{-1} confirm the presence of oxygen-containing groups of C-O stretching bonds [42]. The C-C stretching vibration peaks in the biochar between 1350 and 1600 cm^{-1} provide the presence of aromatics and alkanes [60]. The peaks between 3000 and 3600 cm^{-1} allocated to the O-H functional group it indicates the presence of hydroxyl groups [43]. The peak at 1510 cm^{-1} is due to the aromatic group vibration that confirms the presence of lignin [61]. The peak at 1396 cm^{-1} is originated due to the C-H bending vibration and the existence of alkanes [62]. It is found from there that bio-char loses aliphatic and hydroxyl groups significantly and gains aromatic group.

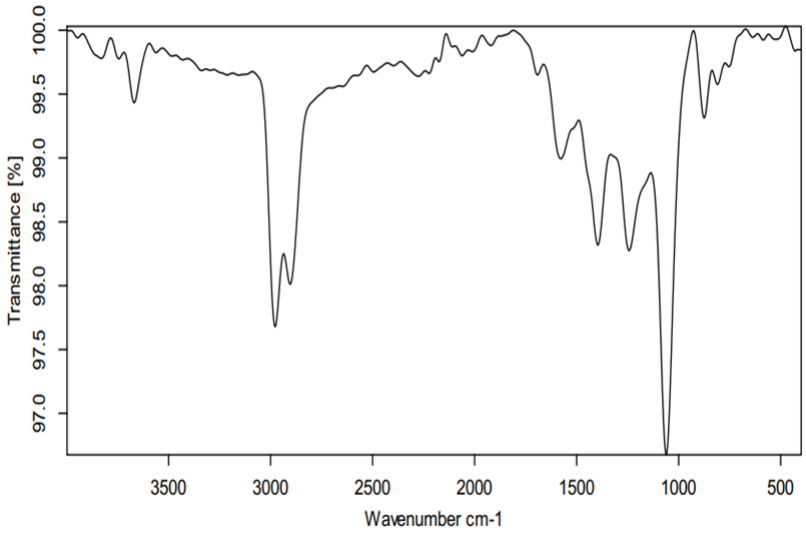

Fig. 9. FTIR spectra of bio-char

The XRD analysis is used to verify the crystallinity of the char [63]. Figure 10 (a) and (b) shows the XRD patterns of sawdust and biochar, respectively, which two sharp peaks at 2θ of around 16 and 22 for sawdust. This determines the presence in biomass of a crystalline cellulose region [64]. However, hemicellulose and lignin are also present in biomass, but they are amorphous in nature. Bio-char partially loses the crystalline structure of cellulose after sawdust pyrolysis so that the crystallinity peak of cellulose also disappears, as shown in Figure 10 (b). This shows cellulose degradation during the process of pyrolysis.

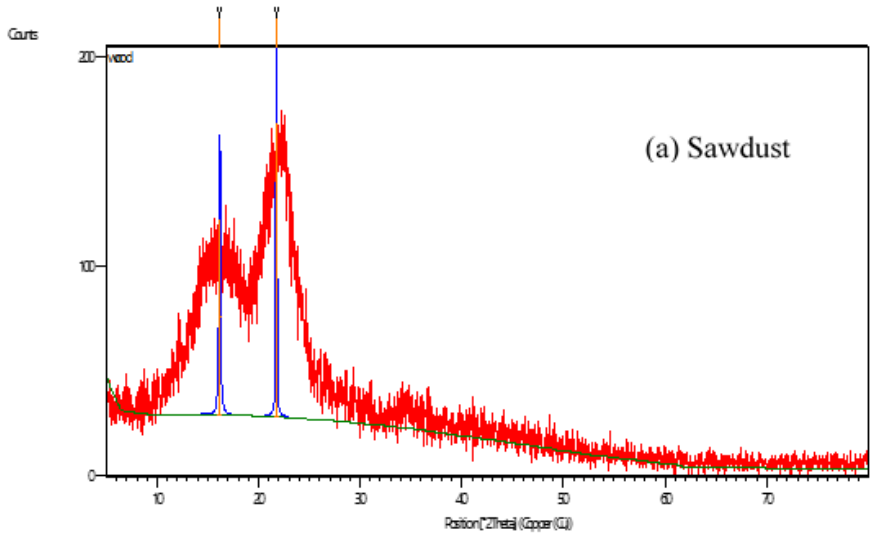

Fig. 10. X-Ray Diffractogram of (a) sawdust

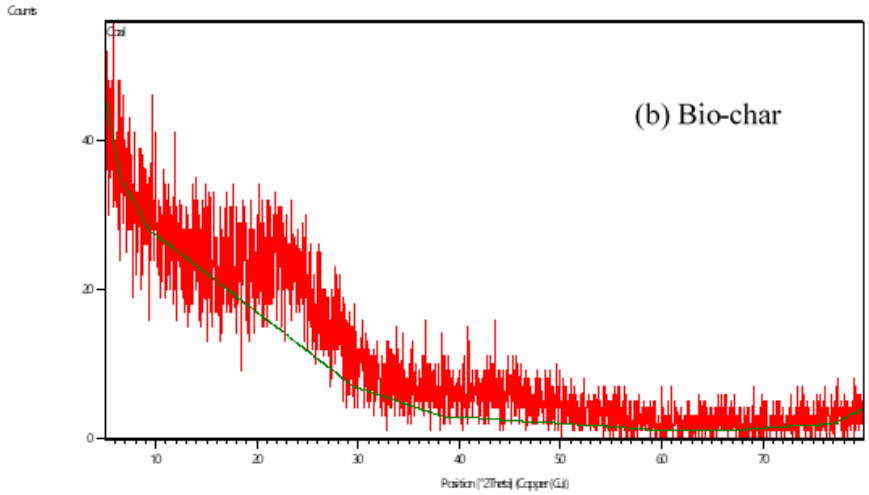

Fig. 10. X-Ray Diffractogram of (b) bio-char

The morphology of the surface of the studied sawdust and bio-char is described by the SEM image, as shown in Figure 11 (a) and (b).

Fig. 11. SEM images of (a) sawdust

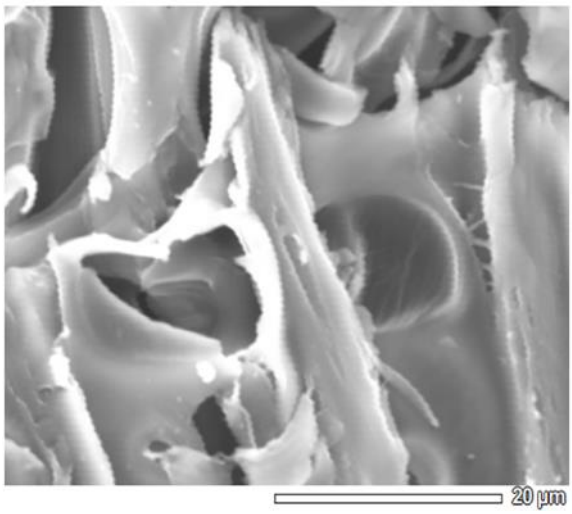

Fig. 11. SEM images of (b) bio-char

In comparing both images, significant different structural surface morphology can be seen. The surface of the sawdust (Fig. 11(a)) is in the form of fibers in one direction, which is the typical case of all cellulosic matters. However, after the pyrolysis, the SEM image of biochar (Fig. 11(b)) exhibits a heterogeneous structure due to the removal of the volatile matters from sawdust during pyrolysis, which leads to the formation of pores at the surface of the bio-char [65]. Highly porous char has a greater number of adsorption sites for ions that offer spaces for water and nutrients/pollutants retention. Figure 12 (a) and (b) represents the EDX analysis of the sawdust and bio-char. It is observed that the bio-char consists of various inorganic matters such as Mg, K, and Ca, and these are the important nutrients for agriculture and to improve crop production [66-67]. Hence, it can also be used as a fertilizer.

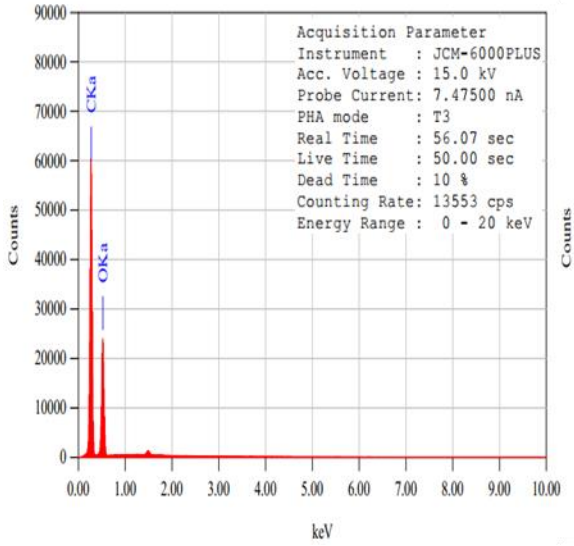

Fig. 12. EDX analysis of (a) sawdust

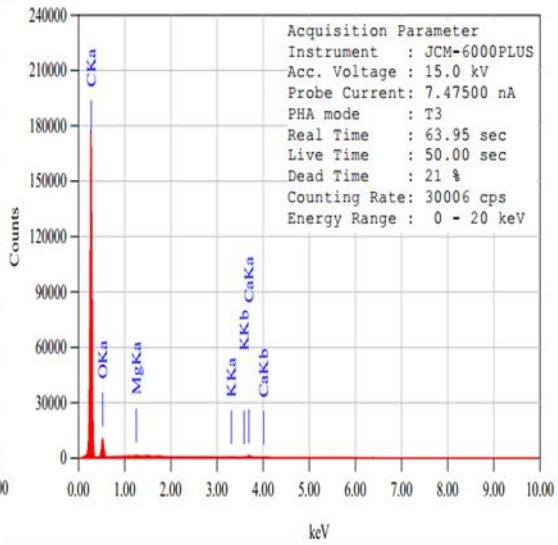

Fig. 12. EDX analysis of (b) bio-char

4.2.7. Comparison between the present study and other literature

Table 5 compares the optimum operating parameters obtained from this study with previous works. It is noticeable that at for a semi-batch pyrolizer and at lower operating temperature (450°C), the yield was 46 wt%, which is higher than obtained by Varma *et al.* [19], but still lower than that obtained by Rout *et al.* [68]. The variation in the yield of bio-oil may be due to variations in the properties of biomass as well as operating parameters. Table 6 compared the CHNS analysis, fuel, and physical properties of this work and others' work.

Table 5. Comparing results for pyrolysis of sawdust with others at different types of forest biomass

Type of biomass	Reactor type	Temperature (°C)	Particle size (mm)	N_2 flow rate (cm^3/min)	Bio-oil yield (wt%)	References
Mixed wood sawdust	Semi batch	450	0.5 - 1	200	46	Present study
Wood sawdust	Fixed bed	550	<1	--	46	[69]
Wood sawdust	Semi batch	500	0.6-1	100	44.16	[19]
Paulownia wood	Fixed bed	550	0.425-1	100	54	[70]
Coconut shell	Semi batch	575	<1	---	49.5	[68]
Perennial grass	Fixed bed	500	0.2	150	26.81	[42]
Napier grass stem	Fixed bed	600	0.2-2	30	32.26	[71]
Olive bagasse	Fixed bed	500	0.425-0.6	150	37.7	[72]

It is clear that the bio-oil produced in the present study has relatively higher carbon, hydrogen, and lower oxygen content than most other studies. In addition, the HHV is analogous to the other bio-oils. Furthermore, the present bio-oil contains lower values of N and S than most bio-oils. Hence, the present process is highly competitive with the others and shows better bio-oil features.

Table 6. A comparison of elemental analysis and fuel properties of sawdust bio-oil with other pyrolytic oils and petroleum product

Pyrolysis bio-oil	Properties									
	Ultimate analysis of bio-oil (%)					HHV (MJ/kg)	Kinematic viscosity at 40°C in cSt	Density at 15°C (kg/m^3)	pH	References
	C	H	N	S	O					
Wood Saw-dust	66.28	6.98	0.76	0.04	25.94	28.45	10.54	1085	3.4	Present study
Wood saw-dust	60.01	6.74	--	--	33.16	26.3	--	--	--	[69]
Wood saw-dust	58.23	7.13	0.70	--	33.94	27.82	16.53	1083	2.6	[19]
Paulownia wood	66.12	8.67	--	--	25.21	28.6	--	--	--	[70]
Coconut shell	59.14	5.47	4.21	0.34	30.84	19.75	1.47	1053.6	--	[68]
Perennial grass	47.95	7.23	0.3	--	44.52	24.7	--	915	3.8	[42]
Napier grass stem	27.5	9.57	0.84	0.14	24.7	25.3	2.45	1030	2.4	[71]
Olive bagasse	66.9	9.2	2	--	21.9	31.8	--	1070	--	[72]
Diesel	85.72	13.2	0.18	0.3	0.6	42- 45	2 - 5.5	820-850	5.6	[68]

5. Conclusions

In this study, a set of pyrolysis experiments were carried out on mixed wood sawdust in a semi-batch reactor to study the effect of pyrolysis temperature, particle size, and purge gas flow rate on product yields. The experimental results showed that at a temperature of 450°C, the particle size of 0.5<Dp<1 mm with a nitrogen flow rate of 200 cm^3/min, the highest bio-oil yield of 46 wt% was obtained. The bio-oil has an empirical formula of $CH_{1.27}O_{0.29}N_{0.009}$ and HHV of 28.45 MJ/kg, and these values are very similar to that of light and heavy liquid fuels. Spectroscopic and chromatographic results suggest the presence in bio-oil of Aliphatic, Aromatic, and Olefinic Hydrocarbons as well as many Oxygenated compounds. After upgrading and refining, this bio-oil can be used for fuel applications. It also can be used as a feedstock for the production of valuable chemicals. Bio-char has a higher carbon content (75.87%) and lower sulfur content (0.03%) and nitrogen content (1.04%) with HHV of 35.428 MJ/kg. It can thus be used as a solid fuel and as a precursor for activated carbon production. SEM and EDX analysis showed that biochar could be used as an adsorbent in the process of water purification and soil nutrient supply. The gaseous products contain carbon monoxide, which can be used as fuel or to be synthesized into fuels.

References

[1] Demirbas A, and Arin G. An Overview of Biomass Pyrolysis. Energy Sources, 2002; 24: 471-482.

[2] Mante OD, and Agblevor FA. Parametric study on the pyrolysis of manure and wood shavings. Biomass and Bioenergy, 2011; 35: 4417-4425.

[3] Moralı U, Yavuzel N, and Şensöz S. Pyrolysis of hornbeam (*Carpinus betulus*, L.) sawdust: Characterization of bio-oil and bio-char. Bioresource Technology, 2016; 221: 682-685.

[4] Zhang X, Deng H, Hou X, Qiu R, and Chen Z. Pyrolytic behavior and kinetic of wood sawdust at isothermal and non-isothermal conditions. Renewable Energy,2019; 142: 284-294.

[5] Li R, Zeng K, Soria J, Mazza G, Gauthier D, Rodriguez R, Flamant G. Product distribution from solar pyrolysis of agricultural and forestry biomass residues. Renewable Energy, 2016; 89: 27-35.

[6] Biswas B, Pandey N, Bisht Y, Singh R, Kumar J, and Bhaskar T. Pyrolysis of agricultural biomass residues: Comparative study of corn cob, wheat straw, rice straw and rice husk. Bioresource Technology, 2017; 237: 57-63.
[7] Tinwala F, Mohanty P, Parmar S, Patel A, and Pant KK. Intermediate pyrolysis of agro-industrial biomasses in bench-scale pyrolyser: Product yields and its characterization. Bioresource Technology, 2015; 188: 258-264.
[8] Wang W-C and Lee A-C. The study of producing "drop-in" fuels from agricultural waste through fast pyrolysis and catalytic hydro-processing. Renewable Energy, 2019; 133: 1-10.
[9] Önal EP, Uzun BB, and Pütün AE. Steam pyrolysis of an industrial waste for bio-oil production. Fuel Processing Technology, 2011; 92: 879-885.
[10] Kar Y. Catalytic pyrolysis of car tire waste using expanded perlite. Waste Management, 2011; 31: 1772-1782.
[11] Bertero M, Gorostegui HA, Orrabalis CJ, Guzmán CA, Calandri EL, and Sedran U. Characterization of the liquid products in the pyrolysis of residual chañar and palm fruit biomasses. Fuel, 2014; 116: 409-414.
[12] Chen W, Shi S, Zhang J, Chen M, and Zhou X. Co-pyrolysis of waste newspaper with high-density polyethylene: Synergistic effect and oil characterization. Energy Conversion and Management, 2016; 112: 41-48.
[13] Miskolczi N, Borsodi N, Buyong F, Angyal A, and Williams P. Production of pyrolytic oils by catalytic pyrolysis of Malaysian refuse-derived fuels in continuously stirred batch reactor. Fuel Processing Technology, 2011; 92: 925-932.
[14] Hwang I-H, Kobayashi J, and Kawamoto K. Characterization of products obtained from pyrolysis and steam gasification of wood waste, RDF, and RPF. Waste management, 2014; 34: 402-410.
[15] Boateng A, Jung H, and Adler P Pyrolysis of energy crops including alfalfa stems, reed canarygrass, and eastern gamagrass. Fuel, 2006; 85: 2450-2457.
[16] Gerçe HF. Bio-oil production from *Onopordum acanthium*, L. by slow pyrolysis. Journal of Analytical and Applied Pyrolysis,2011; 92: 233-238.
[17] McKendry P. Energy production from biomass (part 2): conversion technologies. Bioresource Technology, 2002; 83: 47-54.
[18] Bridgwater AV, Meier D, and Radlein D. An overview of fast pyrolysis of biomass. Organic Geochemistry, 1999; 30: 1479-1493.
[19] Varma AK, Thakur LS, Shankar R, and Mondal P. Pyrolysis of wood sawdust: Effects of process parameters on products yield and characterization of products. Waste Management, 2019; 89: 224-235.
[20] Bhattacharjee N and Biswas AB. Pyrolysis of orange bagasse: Comparative study and parametric influence on the product yield and their characterization. Journal of Environmental Chemical Engineering, 2019; 7: 102903.
[21] Salehi E, Abedi J, and Harding T. Bio-oil from Sawdust: Pyrolysis of Sawdust in a Fixed-Bed System. Energy & Fuels, 2009; 23: 3767-3772.
[22] Demirbaş A. Relationship between Initial Moisture Content and the Liquid Yield from Pyrolysis of Sawdust. Energy Sources, 2005; 27: 823-830.
[23] Aguado R, Olazar M, San José MJ, Aguirre G, and Bilbao J. Pyrolysis of Sawdust in a Conical Spouted Bed Reactor. Yields and Product Composition. Industrial & Engineering Chemistry Research, 2000; 39: 1925-1933.
[24] Varma AK and Mondal P. Physicochemical characterization and kinetic study of pine needle for pyrolysis process. Journal of Thermal Analysis and Calorimetry, 2016; 124: 487-497.
[25] Varma AK and Mondal P. Physicochemical characterization and pyrolysis kinetic study of sugarcane bagasse using thermogravimetric analysis. Journal of Energy Resources Technology,2016; 138: 052205.
[26] Asadullah M, Rahman MA, Ali MM, Rahman MS, Motin MA, Sultan MB, Alam MR, and. Rahman MS. Production of bio-oil from fixed bed pyrolysis of bagasse. Fuel, 2007; 86: 2514-2520.
[27] Cuiping L, Chuangzhi W, and Haitao H. Chemical elemental characteristics of biomass fuels in China. Biomass and bioenergy, 2004; 27: 119-130.
[28] Czajczyńska D, Anguilano L, Ghazal H, Krzyżyńska R, Reynolds AJ, Spencer N, Jouhara H.Potential of pyrolysis processes in the waste management sector. Thermal Science and Engineering Progress, 2017; vol. 3: 171-197.
[29] Nyakuma BB, Johari A, Ahmad A, and Abdullah T. Thermogravimetric analysis of the fuel properties of empty fruit bunch briquettes. Carbon, 2014; 43: 46-62
[30] Chutia RS, Kataki R, and Bhaskar T. Thermogravimetric and decomposition kinetic studies of *Mesua ferrea*, L. deoiled cake. Bioresource Technology, 2013; 139: 66-72.

[31] Bilba K and Ouensanga A. Fourier transform infrared spectroscopic study of thermal degradation of sugar cane bagasse. Journal of Analytical and Applied Pyrolysis, 1996; 38: 61-73.
[32] Shadangi KP and Mohanty K. Kinetic study and thermal analysis of the pyrolysis of non-edible oilseed powders by thermogravimetric and differential scanning calorimetric analysis. Renewable Energy, 2014; 6: 337-344.
[33] Asadieraghi M and Daud WMA. Characterization of lignocellulosic biomass thermal degradation and physiochemical structure: Effects of demineralization by diverse acid solutions. Energy Conversion and Management, 2014; 82: 71-82.
[34] Ghosh MK, and Ghosh UK. Utilization of pine needles as bed material in solid state fermentation for production of lactic acid by lactobacillus strains. BioResources, 2011; 6: 1556-1575.
[35] Guo F, Li X, Wang Y, Liu Y, Li T, and Guo C. Characterization of Zhundong lignite and biomass co-pyrolysis in a thermogravimetric analyzer and a fixed bed reactor. Energy, 2017; 141: 2154-2163.
[36] Wang Z, Cao J, and Wang J. Pyrolytic characteristics of pine wood in a slowly heating and gas sweeping fixed-bed reactor. Journal of Analytical and Applied Pyrolysis, 2009; 84: 179-184.
[37] Cruz G, Braz CE, Ferreira SL, dos Santos AM, and Crnkovic PM Physicochemical Properties of Brazilian Biomasses: Potential Applications as Renewable Energy Source. in 22nd International Congress of Mechanical Engineering (COBEM 2013), Ribeirao Preto, Brazil, Nov, 2013, pp. 3-7.
[38] Zhao Y, Ding M, Dou Y, Fan X, Wang Y, and Wei X. Comparative study on the pyrolysis behaviors of corn stalk and pine sawdust using TG-MS. Transactions of Tianjin University, 2014; 20: 91-96.
[39] Wang T, Ai Y, Peng L, Zhang R, Lu Q, and Dong C. Pyrolysis characteristics of poplar sawdust by pretreatment of anaerobic fermentation. Industrial Crops and Products, 2018; 125: 596-601.
[40] Yang H, Yan R, Chen H, Lee DH, Liang DT, and Zheng C. Mechanism of Palm Oil Waste Pyrolysis in a Packed Bed. Energy & Fuels, 2006; 20: 1321-1328.
[41] Carvalho WS, Cunha IF, Pereira MS, and Ataíde CH. Thermal decomposition profile and product selectivity of analytical pyrolysis of sweet sorghum bagasse: Effect of addition of inorganic salts. Industrial Crops and Products,2015; 74: 372-380.
[42] Saikia R, Chutia RS, Kataki R, and Pant KK. Perennial grass (*Arundo donax* L.) as a feedstock for thermo-chemical conversion to energy and materials. Bioresource Technology, 2015; 188: 265-272.
[43] Yang H, Yan R, Chen H, Lee DH, and Zheng C. Characteristics of hemicellulose, cellulose and lignin pyrolysis. Fuel, 2007; 86: 1781-1788.
[44] Isahak WNRW, Hisham MWM, Yarmo MA, and Yun Hin T-Y. A review on bio-oil production from biomass by using pyrolysis method. Renewable and Sustainable Energy Reviews, 2012; 16: 5910-5923.
[45] Haykiri-Acma H. The role of particle size in the non-isothermal pyrolysis of hazelnut shell. Journal of Analytical and Applied Pyrolysis, 2006; 75: 211-216.
[46] Uzun BB, Pütün AE, and Pütün E. Fast pyrolysis of soybean cake: Product yields and compositions. Bioresource Technology, 2006; 97: 569-576.
[47] Moralı U and Şensöz S. Pyrolysis of hornbeam shell (*Carpinus betulus* L.) in a fixed bed reactor: Characterization of bio-oil and bio-char. Fuel, 2015; 150: 672-678.
[48] Özçimen D, and Karaosmanoğlu F. Production and characterization of bio-oil and biochar from rapeseed cake. Renewable Energy, 2004; 29: 779-787
[49] Sukumar V, Manieniyan V, Senthilkumar R, and Sivaprakasam S. Production of Bio Oil from Sweet Lime Empty Fruit Bunch by Pyrolysis. Renewable Energy, 2020; 146: 309-3015.
[50] Abnisa F, Arami-Niya A, Daud WMAW, Sahu JN, and Noor IM. Utilization of oil palm tree residues to produce bio-oil and bio-char via pyrolysis. Energy Conversion and Management, 2013; 76: 1073-1082.
[51] Varma AK, and Mondal P. Pyrolysis of sugarcane bagasse in semi batch reactor: Effects of process parameters on product yields and characterization of products. Industrial Crops and Products, 2017; 95: 704-717.
[52] Jeong YW, Choi SK, Choi YS, and Kim SJ. Production of biocrude-oil from swine manure by fast pyrolysis and analysis of its characteristics. Renewable Energy, 2015; 79: 14-19.
[53] Islam MN, Zailani R, and Ani FN. Pyrolytic oil from fluidised bed pyrolysis of oil palm shell and itscharacterisation. Renewable Energy, 1999; 17: 73-84.
[54] Tsai WT, Lee MK, and Chang YM. Fast pyrolysis of rice straw, sugarcane bagasse and coconut shell in an induction-heating reactor. Journal of Analytical and Applied Pyrolysis, 2006; 76: 230-237.

[55] Bordoloi N, Narzari R, Sut D, Saikia R, Chutia RS, and Kataki R. Characterization of bio-oil and its sub-fractions from pyrolysis of *Scenedesmus dimorphus*. Renewable Energy, 2016; 98: 245-253.
[56] Garg R, Anand N, and Kumar D. Pyrolysis of babool seeds (*Acacia nilotica*) in a fixed bed reactor and bio-oil characterization. Renewable Energy, 2016; 96: 167-171.
[57] Liu Q, Liu P, Xu Z-X, He Z-X, and Wang Q. Bio-fuel oil characteristic of rice bran wax pyrolysis. Renewable Energy, 2018; 119: 193-202.
[58] Singh VK, Soni AB, Kumar S, and Singh RK. Pyrolysis of sal seed to liquid product. Bioresource Technology, 2014; 151: 432-435.
[59] Yakub MI, Abdalla AY, Feroz KK, Suzana Y, Ibraheem A, and Chin SA. Pyrolysis of oil palm residues in a fixed bed tubular reactor. Journal of Power and Energy Engineering, 2015; 3: 185.
[60] Aysu T. Catalytic pyrolysis of *Eremurus spectabilis* for bio-oil production in a fixed-bed reactor: Effects of pyrolysis parameters on product yields and character. Fuel Processing Technology, 2015; 129: 24-38.
[61] Xu S, Uzoejinwa BB, Wang S, Hu Y, Qian L, Liu L, Li B, He Zh, Wang Q, Abomohra AE, Li Ch, Zhang B. Study on co-pyrolysis synergistic mechanism of seaweed and rice husk by investigation of the characteristics of char/coke. Renewable Energy, 2019; 132: 527-542.
[62] Balagurumurthy B, Srivastava V, Vinit RJ, Kumar J, Biswas B, Singh R, Gupta P, Kumar KL, Singh R, Bhaskar T. Value addition to rice straw through pyrolysis in hydrogen and nitrogen environments. Bioresource Technology, 2015; 188: 273-279.
[63] M Ertaş and M. Hakkı Alma Pyrolysis of laurel (*Laurus nobilis* L.) extraction residues in a fixed-bed reactor: Characterization of bio-oil and bio-char. Journal of Analytical and Applied Pyrolysis, vol. 88, pp. 22-29, 2010/05/01/ 2010.
[64] Z-H Jiang, Z Yang, C-. So, and C-Y. Hse, Rapid prediction of wood crystallinity in *Pinus elliotii* plantation wood by near-infrared spectroscopy. Journal of Wood Science, vol. 53, pp. 449-453, 2007/10/01 2007.
[65] Yao Y, Gao B, Inyang M, Zimmerman AR, Cao X, Pullammanappallil P, Yang L. Biochar derived from anaerobically digested sugar beet tailings: Characterization and phosphate removal potential. Bioresource Technology, 2011; 102: 6273-6278.
[66] Chutia RS, Kataki R, and Bhaskar T. Characterization of liquid and solid product from pyrolysis of Pongamia glabra deoiled cake. Bioresource Technology, 2014; 165: 336-342.
[67] KH Kim, T-S Kim, S-M Lee, D Choi, H Yeo, I-G Choi, Choi JW. Comparison of physicochemical features of biooils and biochars produced from various woody biomasses by fast pyrolysis. Renewable Energy, 2013; 50: 188-195.
[68] Rout T, Pradhan D, Singh RK, and Kumari N. Exhaustive study of products obtained from coconut shell pyrolysis. Journal of Environmental Chemical Engineering, 2016; 4: 3696-3705.
[69] Özbay G, Pekgözlü AK, and Ozcifc A. The effect of heat treatment on bio-oil properties obtained from pyrolysis of wood sawdust. European Journal of Wood and Wood Products, 2015; 73: 507-514.
[70] Yorgun S, and Yıldız D. Slow pyrolysis of paulownia wood: Effects of pyrolysis parameters on product yields and bio-oil characterization. Journal of Analytical and Applied Pyrolysis, 2015; 114: 68-78.
[71] Mohammad I, Abakr Y, Kabir F, Yusuf S, Alshareef I, and Chin S. Pyrolysis of Napier grass in a fixed bed reactor: effect of operating conditions on product yields and characteristics. BioResources, 2015; 10: 6457-6478.
[72] Şensöz S, Demiral İ, and Ferdi Gerçel H. Olive bagasse (Olea europea L.) pyrolysis. Bioresource Technology, 2006; 97: 429-436.

To whom correspondence should be addressed: Dr. Ahmed Gaber H. Saif, Dept. of Mechanical Power Engineering and Energy, Faculty of Engineering, Minia University, Minia 61519, Egypt, E-mail: Ahmed.gaber52@mu.edu.eg